iScience

CellPress
OPEN ACCESS

Article

# Rapid hydrolysis rates of thio- and phosphate esters constrain the origin of metabolism to cool, acidic to neutral environments

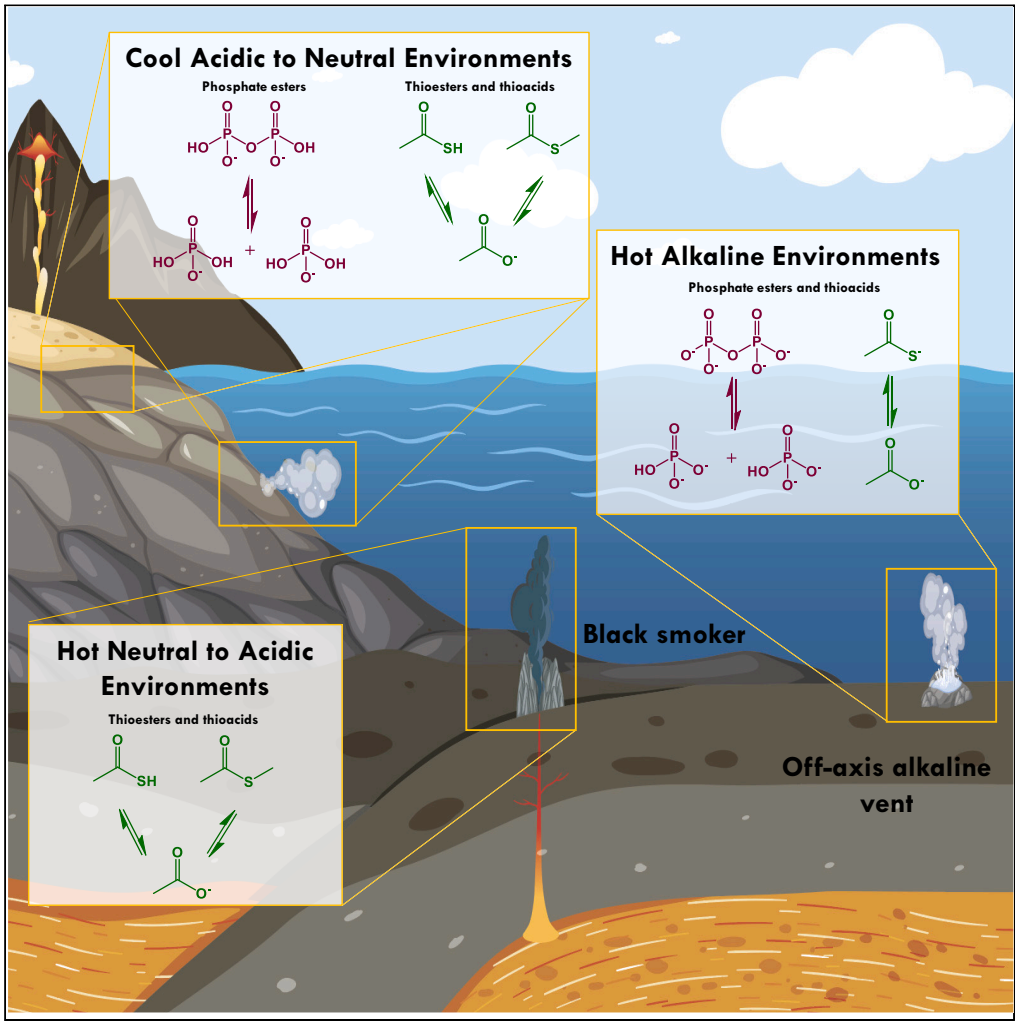


Sebastian A. Sanden, Christopher J. Butch, Stuart Bartlett, Nathaniel Virgo, Yasuhito Sekine, Shawn Erin McGlynn

sebastian.sanden@rub.de (S.A.S.)
chrisbutch@nju.edu.cn (C.J.B.)
mcglynn@elsi.jp (S.E.M.)

## Highlights

Free energy is calculated using experimental hydrolysis rates and computed energies

Energy availability is constrained by ester hydrolysis rates, not free energies

The highest stability of S- and P-esters coincides with geochemical abundance

Sanden et al., iScience 27, 111088
November 15, 2024 
https://doi.org/10.1016/j.isci.2024.111088

iScience

CellPress
OPEN ACCESS

Article

# Rapid hydrolysis rates of thio- and phosphate esters constrain the origin of metabolism to cool, acidic to neutral environments

Sebastian A. Sanden,[1,2,*] Christopher J. Butch,[1,3,*] Stuart Bartlett,[1,4] Nathaniel Virgo,[1] Yasuhito Sekine,[1,5,6] and Shawn Erin McGlynn[1,7,8,9,*]

## SUMMARY

**Universal to all life is a reliance on energy carriers such as adenosine triphosphate (ATP) which connect energy-releasing reactions to energy-consuming processes. While ATP is ubiquitously used today, simpler molecules such as thioesters and polyphosphates are hypothesized to be primordial energy carriers. Investigating environmental constraints on the non-enzymatic emergence of metabolism, we find that hydrolysis rates—not hydrolysis energies—differentiate phosphate esters and thioesters. At temperatures consistent with thermophilic microbes, thioesters are favored at acidic pH and phosphate esters at basic pH. Thioacids have a high stability across pH 5–10. The planetary availability of sulfur and phosphate is coincident with these calculations, with phosphate being abundant in alkaline and sulfur in acidic environments. Since both sulfur esters and phosphate esters are uniquely required in metabolism, our results point to a non-thermophilic origin of early metabolism at cool, acidic to neutral environments.**

## INTRODUCTION

Cellular replication is predicated on chemical energy conversion. In today's metabolisms, universal metabolic energy carriers in the form of phosphoesters and thioesters, such as adenosine triphosphate (ATP) and acetyl-coenzyme A (CoA), are used to harness chemical potential. This chemical potential is then used to activate monomers prior to polymerization, and also to drive key protein conformational changes in a wide array of processes ranging from electron transfer in nitrogenase[1] to movement of myosin.[2,3]

The crucial roles of these energy carriers today make them key to our understanding of the origin of life. Biological energy carrier formation today is driven largely by electron transfer reactions in respiration coupled to chemiosmosis and also involves substrate-level phosphorylation.[4] A diversity of abiotic, non-enzymatic routes for ester synthesis have been demonstrated experimentally including dry-down[5–7]; heating of phosphates Ca $(HPO_4)_2$ [8,9]; thioacid and thioester formation from COS or CO[10–12]; redox neutral reactions involving aldehydes, keto acids, and light[13,14]; and also nitrile hydrolysis leading to phosphoesters, thioesters, and thioacids.[15–17] High group transfer potential of prebiotic relevance has also come into view from chemistry involving trimetaphosphate, diamidophosphate,[18,19] and thioformamide.[20] This array of synthetic paths and the molecular diversity they afford suggest that multiple types of molecules with high group transfer potential may have been available to early metabolism.

Arguments have been made for life's emergence with one type of energy carrier molecule, with later diversification into others; for example, in De Duve's "thioester world" life would have started by using thioesters and later phosphate esters would have been recruited into metabolism,[21] a notion bolstered by the observation of thioester stability at 25°C and rapid thiol exchange which could have been involved in an early energy economy.[22] These molecules may have taken part in early energy exchange reactions, some of which are illustrated in Figure 1, which shows experimentally demonstrated interconversion of sulfur-based energy carriers into phosphoanhydrides and peptides. Regardless of the specific type of molecule, the high group transfer potential of energy carriers makes them susceptible to spontaneous hydrolysis, necessitating continuous synthesis. Water is the numerically major metabolite of a cell today,[23] and its involvement in metabolic evolution is a constraint to be considered.[24]

[1]Earth Life Science Institute, Tokyo Institute of Technology, 2-12-1 I7E Ookayama, Meguro, Tokyo 152-8550, Japan
[2]Inorganic Chemistry I, Ruhr-University Bochum, Universitaetsstrasse 150, 44801 Bochum, Germany
[3]Department of Biomedical Engineering, College of Engineering and Applied Sciences, Nanjing University, Nanjing 210023, China
[4]Division of Geological and Planetary Sciences, California Institute of Technology, Pasadena, CA 91125, USA
[5]Institute of Nature and Environmental Technology, Kanazawa University, Ishikawa, Japan
[6]Planetary Plasma and Atmospheric Research Center, Tohoku University, Miyagi, Japan
[7]Blue Marble Space Institute of Science, Seattle, WA, USA
[8]Biofunctional Catalyst Research Team, RIKEN Center for Sustainable Resource Science, Wako, Japan
[9]Lead contact
*Correspondence: sebastian.sanden@rub.de (S.A.S.), chrisbutch@nju.edu.cn (C.J.B.), mcglynn@elsi.jp (S.E.M.)
https://doi.org/10.1016/j.isci.2024.111088

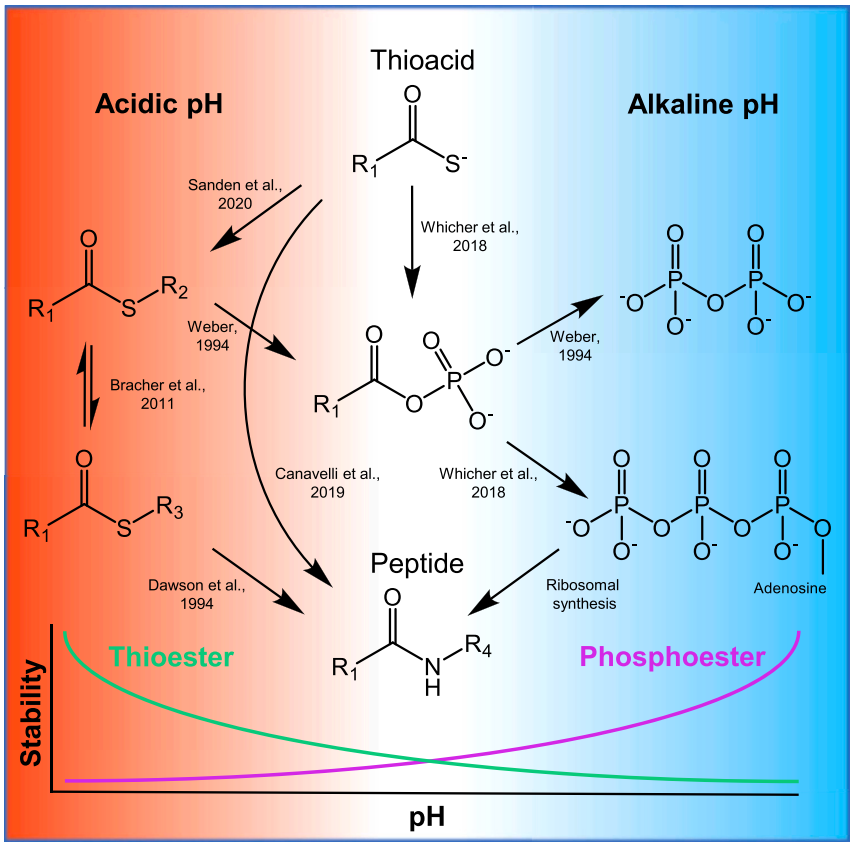


**Figure 1. Network of possible interconversions between thioacids, thioesters, peptides and phosphoesters**

Acidic environments at thermophilic growth temperatures (>65°C or 340 K) favor thioesters as energy carriers due to an increased stability, whereas phosphoesters are more stable at alkaline conditions and thioacids tolerate both acidic and alkaline pH. The reaction arrows also include labels with the names of the corresponding authors and the year of publication.[14,17,22,25–27]

Here we integrated kinetic and thermodynamic data on thioacids, thioesters, and phosphoesters to uncover environmental constraints on energy conversion at the origin of life. Experimental reaction rates are combined with hydrolytic energies computed by density functional theory (DFT), and the available energy is discussed with respect to the stability of each ester from pH 5–10 and temperatures of 300–400 K. Based on these energy constraints, possible geochemical scenarios are discussed, in the context of the origin of metabolism occurring in thermophilic settings (>65°C) or at cooler temperatures.

## RESULTS

Biological growth extends from below zero to above 100°C.[28–30] Genome comparison studies show that the reverse gyrase gene can be used as a marker of growth ability above 65°C, establishing this temperature as a natural boundary for considering what constitutes "hot" for life.[31–34] Here we are concerned with the non-enzymatic emergence of group transfer potential and discuss the results above and below the reverse gyrase-established temperature, which is approximately 340 K.

### Temperature- and pH-dependent hydrolysis kinetics

Hydrolysis energies are similar between thioesters, thioacids, and phosphate esters (cf. Table S2); however, reaction rates at the same temperature differ by orders of magnitude between the esters, indicating that kinetics are the deciding factor for energy availability. Figure 2 displays the spread of measured hydrolysis rates and shows differences up to $10^5$ $s^{-1}$ for the hydrolysis rates of the thioester methyl-thioacetate (MTA), thioacetic acid (TAA), diphosphate (PP) and triphosphate (PPP), and ATP to ADP at pH 5, 7, and 10. The pseudo first-order hydrolysis rate constants were extrapolated for a given pH from experimental results[35–38] and are supplemented here in the case of MTA and TAA by new $^1$H-nuclear magnetic resonance (NMR) data at 4 different temperatures at pH 5.

At temperatures < 50° C and between pH 5 and 7, the hydrolysis rates have a spread of about $10^2$ $s^{-1}$, but, if we consider hyperthermophilic growth temperatures above 65°C, the thioester MTA is most stable at pH 5, and the thioacid TAA at pH 7. This higher stability of thioesters at high temperature and acidic pH is coincident with De Duve's proposal that thioesters might have been the primordial energy carrier and have operated in a hot acidic environment.[21] But the advantage of thioesters disappears at alkaline pH, as MTA hydrolysis is base catalyzed.[22] At a

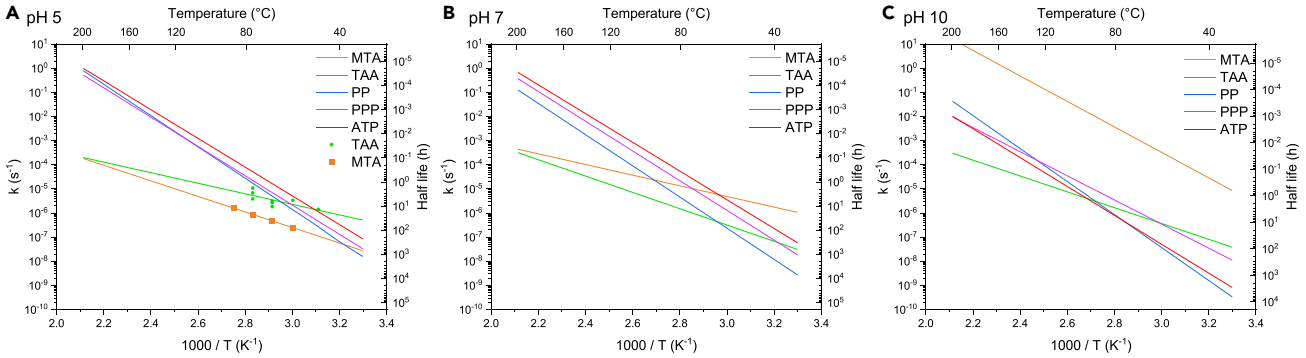


**Figure 2. Hydrolysis rates and half-lives of methyl-thioaceate, thioacetic acid, pyrophosphate, triphosphate, and adenosine triphosphate**

The hydrolysis rates at pH 5 (A), pH 7 (B), and pH 10 (C) plotted on a log base 10 scale vs. 1,000/T in K. The hydrolysis rates of MTA and TAA were measured via $^{1}$H-NMR in a 100 mM citric acid buffer at pH 5 and are indicated as points in (A). $r^2$ of the residual sum of squares method was 0.99 for MTA and 0.56 for TAA. The hydrolysis rates for PP, PPP, and ATP are extrapolated from experimental results between 30°C to 120°C found in the literature.[35–38]

temperature of 100°C, the hydrolysis rate of MTA is extrapolated to being 4 orders of magnitude faster than that for TAA at pH 10; which results in a half-life of 43 s for MTA at alkaline hydrothermal conditions, making thioesters an unsuitable energy carrier at alkaline hydrothermal vent conditions.[38] The 46.5 h half-life of TAA is comparable to those of ATP and PP, which are 46 h and 33 h respectively.

From pH 5 to 10, the phosphoesters PP, PPP, and ATP exhibit a similar temperature dependence of their respective hydrolysis rates, which result from similar activation energies for hydrolysis (cf. Table S1). Phosphoesters are not subject to base-catalyzed hydrolysis at pH 10, likely because of coulombic repulsion of the hydroxyl ions due to their negatively charged phosphate residues, and the hydrolysis rates even decrease by an order of magnitude from pH 5 to pH 10. Similarly, the hydrolysis rates of the negatively charged thioacetate ($pk_a$ = 3.3) are largely independent of pH and, while phosphoesters are the most stable compounds until about 100°C (Figure 2C), at higher temperatures and high pH, TAA is hydrolytically more stable. Across the pH conditions surveyed, the thioacid is broadly the most kinetically stable at high temperatures.

## Energy availability from geo-esters

When life began, geochemically produced esters harboring group transfer potential may have provided energy needed for metabolic processes. Such "geo-esters" would have been subjected to water hydrolysis, leaving behind variable amounts of energy depending on the group transfer potential of each molecule and the kinetics of the molecules which might react with them. To gain an understanding of this variability of energy availability from the different esters, we combined kinetic hydrolysis data with thermodynamic information and calculated energy availability over time at variable concentrations, different temperatures, and different pH values. In this model, 1 M is used as the starting concentration for easier connection to other known values at $\Delta G'^{\circ}$.[39] To obtain a consistent set of hydrolysis energies that includes MTA and TAA, for which no experimental data were available, the Gibbs free energies of hydrolysis were computed via DFT using PBE0 6–311(2d,2p), as implemented in Gaussian 16, and the SMD solvation model including implicit solvation. The Gibbs free energy of hydrolysis at a given pH and temperature, which can potentially be coupled to a group transfer reaction, is referred to here as energy availability.

Figure 3 shows the time evolution of energy availability for a thioester, thioacid, and ATP. Although there is variability in group transfer potential between the esters, the primary control in energy availability is hydrolysis rate. The energy demands and required reaction rates of early metabolism are not constrained, but we can consider what we know from contemporary biology: free energies in the range of −10 to −20 kJ mol$^{-1}$ are associated with cellular metabolism, −20 kJ mol$^{-1}$ is needed for transporting a monovalent ion across a charged cellular membrane, and ca. −15 kJ mol$^{-1}$ is needed to promote peptide bond formation.[40–42] In our model, all esters are able to provide at least −20 kJ mol$^{-1}$ at ambient conditions of 300 K (27°C) for up to 900 h, but, at hyperthermophilic temperature of 360 K (87°C) and pH 5, MTA is able to provide −20 kJ mol$^{-1}$ for 420 h, whereas TAA reaches this threshold in 33 h and ATP in less than 6 h. (Figure 3, dashed line). At pH 7 and 360 K (87°C), TAA can provide −20 kJ mol$^{-1}$ for 310 h, but MTA and ATP for less than 20 h. At the hyperthermophilic temperature of 360 K (87°C), thioesters and thioacids can thus provide sufficient free energy for at least ten times longer than ATP at acidic and neutral pH, respectively. In contrast, at 360 K (87°C) and pH 10, ATP can provide −20 kJ mol$^{-1}$ for $10^3$ h, whereas MTA is hydrolyzed after 0.3 h and TAA after 360 h.[38] The increased stability of ATP under alkaline conditions also extends to the inorganic analogs PPs and PPPs, but they are also subjected to rapid hydrolysis at elevated temperatures at pH 7 and below (Figure S1 and Table S2).

# DISCUSSION

## The origin of ester metabolism and its overlaps with planetary geochemistry

pH and temperature are fundamental variables in chemical processes and therefore crucial parameters for life today and its origin.[39,43,44] Using the stability ranges presented herein for energy carriers, we may consider different scenarios for how energy metabolism could have emerged

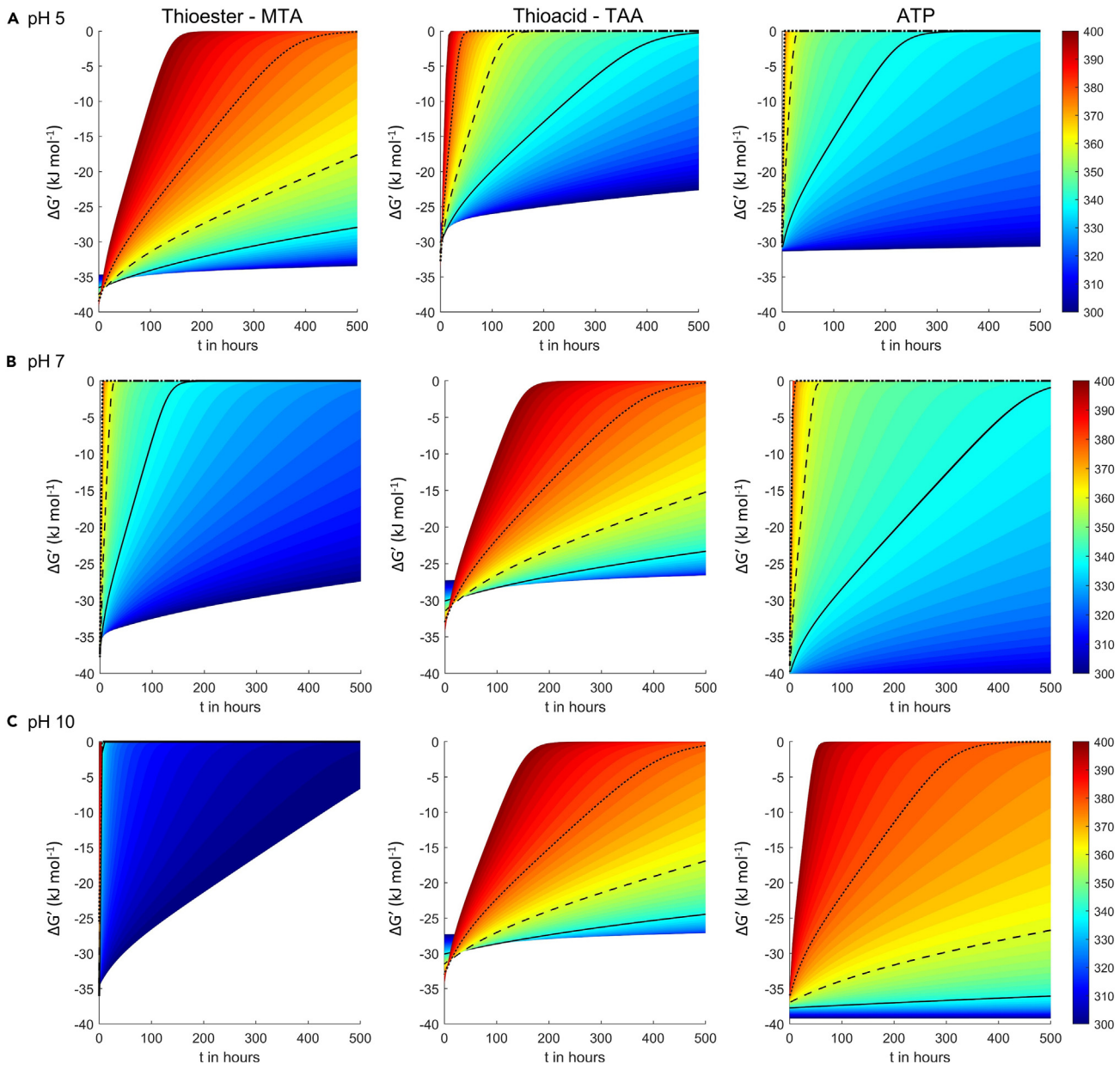


**Figure 3. Gibbs free energy of hydrolysis over time with respect to temperature**

Hydrolysis model depicting the available Gibbs free energy over time with temperature color-coded as a heatmap from 300 to 400 K. (A) depicts the Gibbs free energy at pH 5, (B) at pH 7 and (C) at pH 10. In addition, the available free energy at the lower bound of thermophilic growth temperatures; 340 K (66.85°C) is represented as a solid line, 360 K (86.85°C) as a dashed line, and 380 K (106.85°C) as a dotted line. The available Gibbs free energy of reaction of methylthioacetate, thioacetic acid, and adenosine triphosphate (hydrolyzing to ADP) is given in kJ $mol^{-1}$ with starting concentrations of 1 M for reactants and products in 1 L of water, referring to $\Delta G'^{o}$. Additional details concerning the model are described below.

from geochemistry. If life started in a hot alkaline environment, thioester- and thioacid-based metabolisms would struggle to compete with water hydrolysis and life may have started with a sole reliance on phosphate esters, perhaps as outlined by Russell in a hypothesis involving green rust.[45] However if life started in a hot acidic environment, it may have started with a sole reliance on thioesters; at neutral pH, early thermophilic life may have preferred thioacids. A surface-based metabolism using thioesters and thioacids as proposed by Wächtershäuser, situated in a neutral to acidic sulfide-rich hydrothermal environment, is viable according to the stability ranges of MTA and TAA.[21,46,47]

The fundamental processes of amino acid and nuceleic acid synthesis in extant metabolism rely on the presence of both thioesters and phosphoesters.[48] Based on the thermogeochemical constraints imposed by phosphate and thioester hydrolysis above the thermphilic temperature of 340 K, an origin of life consistent with mesophilic growth of today's organisms, or even a cold origin of life,[49,50] could be more likely

than the higher-temperature scenarios previously considered. Cooler temperatures would have opened the possibility of an ester energy currency economy of the type we see in cells today where interconversions between ester types facilitate the operation of large metabolic networks.

The general availability of sulfur and phosphorous in aqueous environments such as the primordial ocean could further constrain the choice of energy carriers. The results of high stability of phosphate esters in alkaline hydrothermal systems coincide with high availability of dissolved phosphate in geochemistry in the same environments. Under alkaline $CO_2$-rich hydrothermal conditions, calcium phosphate minerals in host rocks are dissolved to form stable Ca-carbonate minerals, releasing dissolved phosphate into fluids.[51–53] Such environments are commonly achieved when ultramafic rocks and $CO_2$-rich water interact, including deep-crustal hydrothermal systems on early Earth[54] and hydrothermal environments of icy ocean worlds in the outer solar system.[53] Given that high concentrations of phosphate are required for phosphorylation of prebiotic molecules,[55] life, if it arose in alkaline waters, could have utilized phosphate esters for early metabolism assuming mechanisms for making use of these compounds were available.

On the other hand, acidic hydrothermal systems tend to appear in sulfur-rich and/or $CO_2$-limited hydrothermal environments.[54,56] Mars—from its core to surface—contains more sulfur than Earth.[57] Sulfur isotopes preserved in lake sediments of Gale Crater suggest that sulfur was highly involved in impact-driven hydrothermal environments on early Mars.[58] In addition, organic matter found in lake sediments of Gale Crater contains a large fraction of sulfur but little phosphate and nitrogen.[59] These findings suggest high geochemical availability and reactivity of sulfur on early Mars, where sulfur-based esters could be preferred for early metabolism of life. Altogether, it appears that the overlap between elemental availability and the energetic characteristics of P and S compounds could have preordained their respective use in thermophilic, hydrothermal conditions >340 K; 65°C.

### Conclusion

The bioenergetics of the cell are organized around the continuous production of group transfer potential, which is key for sustained polymer production and activation reactions required for cell metabolism. Using kinetic calculations and DFT, we demonstrated differences between sulfur acetyl esters and phosphoanhydrides as energy carriers in early metabolism. The stability of these energy carriers constrains their use in nascent metabolism, in particular if the geochemical source producing esters was intermittent or spatially distant.

Since energy conversion processes are universal in biology, we suspect that environmental factors which constrain one molecular type over another could have represented a molecular guide, or filter. Our results suggest that acidic and alkaline environments at elevated temperatures (>340 K; ca. 65°C) favor thioesters or phosphate esters, respectively. If we examine contemporary metabolism, it seems that both sulfur esters and phosphate esters are required for unique cellular processes: if so, our results point to an origin of early metabolism at cool, acidic to neutral environments inconsistent with thermophilic growth.

### Limitations of the study

In this study, we focused solely on hydrolysis rates to gain a picture of energy availability from what we term geo-esters: molecules with a high group transfer potential which may have been produced geochemically. We did not consider formation rates nor coupled reactions which will be necessary to form a more complete model of primordial metabolism. This model does not account for other factors such as metal ions and UV exposure which may accelerate ester hydrolysis.[60] If we look at biology today, we find that life metabolizes and uses energy at rates which differ by orders of magnitude[61]: the energy demands at the origin of life are not known but would influence the considerations brought forward in this paper.

The Gibbs free energies reported here were computed *ab initio* by DFT. The computed reaction energies match well with experimental hydroltic energies; though charged compounds can produce errors up to 10 kcal $mol^{-1}$ without implicit solvation (cf. supplemental information). With hydrolysis rates of S- and P-esters differing by orders of magnitude, the energy availability model may become sensitive to errors concerning the Gibbs free energies of hydrolysis in temperature and pH regimes where the hydrolysis rates are comparable, i.e., within one order of magnitude. Increased precision on the hydrolysis energies in these regimes would improve the model.

The possibility that the first metabolic networks utilized energy carriers different from those discussed here should be considered. Our results argue against the simultaneous use of both phosphate esters and sulfur esters at high temperature: one intriguing idea resulting from this is that if life did begin at high temperature, it may have used different molecular forms of group transfer potential than those seen today and investigated here.

## RESOURCE AVAILABILITY

### Lead contact

Requests for further information and resources should be directed to and will be fulfilled by the lead contact, Shawn E. McGlynn (mcglynn@elsi.jp).

### Materials availability

This study did not generate new materials.

## Data and code availability

- The MATLAB code used for the combined free energy model, including the experimental parameters for each discussed chemical species, is available as of the date of publication.
- All original code has been deposited at Zenodo and is publicly available as of the date of publication. https://doi.org/10.5281/zenodo.10801842.
- Any additional information required to reanalyze the data reported in this paper is available from the lead contact upon request.

## ACKNOWLEDGMENTS

This study was carried out using the TSUBAME 3.0 supercomputer at Tokyo Institute of Technology. S.E.M. acknowledges funding from NSF award no. 1724300 and JSPS KAKENHI grant numbers JP22H01343 and JP22K18278. S.A.S. acknowledges a graduate scholarship received from MEXT of Japan. The authors thank Kuhan Chandru for his assistance on determining the experimental hydrolysis rates. Asset images by brgfx and Freepik on Freepik (www.freepik.com) were used in the generation of the graphical abstract. Contents from this paper were discussed at the "Feasible but Undiscovered Metabolisms: Thermodynamics, Evolution, and the Origin of Life" organized by C. Kempes, C. McShea, and S. McGlynn at the Santa Fe Institute, July 2022.

## AUTHOR CONTRIBUTIONS

S.A.S.: conceptualization, methodology, investigation, visualization, writing – original draft, and writing – review and editing. C.J.B.: methodology, investigation, and writing – review and editing. S.B.: methodology, investigation, and writing – review and editing. N.V.: methodology and writing – review and editing. Y.S.: writing – original draft and writing – review and editing. S.E.M.: conceptualization, supervision, writing – original draft, and writing – review and editing.

## DECLARATION OF INTERESTS

The authors declare no competing interests.

## STAR★METHODS

Detailed methods are provided in the online version of this paper and include the following:



## SUPPLEMENTAL INFORMATION

Supplemental information can be found online at https://doi.org/10.1016/j.isci.2024.111088.

Received: May 9, 2024
Revised: September 12, 2024
Accepted: September 27, 2024
Published: October 3, 2024

## REFERENCES

1. Duval, S., Danyal, K., Shaw, S., Lytle, A.K., Dean, D.R., Hoffman, B.M., Antony, E., and Seefeldt, L.C. (2013). Electron transfer precedes atp hydrolysis during nitrogenase catalysis. Proc. Natl. Acad. Sci. USA *110*, 16414–16419.
2. Astumian, R.D., and Bier, M. (1996). Mechanochemical coupling of the motion of molecular motors to atp hydrolysis. Biophys. J. *70*, 637–653.
3. Fontecilla-Camps, J.C. (2022). The complex roles of adenosine triphosphate in bioenergetics. Chembiochem. *23*, e202200064.
4. Nitschke, W., Schoepp-Cothenet, B., Duval, S., Zuchan, K., Farr, O., Baymann, F., Panico, F., Minguzzi, A., Branscomb, E., and Russell, M.J. (2023). Aqueous electrochemistry: The toolbox for life's emergence from redox disequilibria. Electrochem. Sci. Adv. *3*, e2100192.
5. Mamajanov, I., MacDonald, P.J., Ying, J., Duncanson, D.M., Dowdy, G.R., Walker, C.A., Engelhart, A.E., Fernández, F.M., Grover, M.A., Hud, N.V., and Schork, F.J. (2014). Ester formation and hydrolysis during wet–dry cycles: Generation of far-from-equilibrium polymers in a model prebiotic reaction. Macromolecules *47*, 1334–1343.
6. Forsythe, J.G., Yu, S.-S., Mamajanov, I., Grover, M.A., Krishnamurthy, R., Fernández, F.M., and Hud, N.V. (2015). Ester-mediated amide bond formation driven by wet–dry cycles: A possible path to polypeptides on the prebiotic earth. Angew. Chem. Int. Ed. *54*, 9871–9875.
7. Frenkel-Pinter, M., Bouza, M., Fernández, F.M., Leman, L.J., Williams, L.D., Hud, N.V., and Guzman-Martinez, A. (2022). Thioesters provide a plausible prebiotic path to proto-peptides. Nat. Commun. *13*, 2569. https://doi.org/10.1038/s41467-022-30191-0.
8. Rabinowitz, J., Chang, S., and Ponnamperuma, C. (1968). Phosphorylation on the primitive earth: Phosphorylation by way of inorganic phosphate as a potential prebiotic process. Nature *218*, 442–443.
9. Yamagata, Y., Watanabe, H., Saitoh, M., and Namba, T. (1991). Volcanic production of polyphosphates and its relevance to prebiotic evolution. Nature *352*, 516–519.
10. Leman, L., and Ghadiri, M. (2016). Potentially prebiotic synthesis of α-amino thioacids in water. Synlett *28*, 68–72.
11. Huber, C., and Wächtershäuser, G. (1997). Activated acetic acid by carbon fixation on (Fe, Ni)S under primordial conditions. Science *276*, 245–247.
12. Kitadai, N., Nakamura, R., Yamamoto, M., Okada, S., Takahagi, W., Nakano, Y., Takahashi, Y., Takai, K., and Oono, Y. (2021). Thioester synthesis through geoelectrochemical $Co_2$ fixation on Ni sulfides. Commun. Chem. *4*, 37.
13. Leqraa, N., Nicolet, Y., Milet, A., and Vallée, Y. (2020). A way to thioacetate esters compatible with non-oxidative prebiotic conditions. Sci. Rep. *10*, 14488.
14. Weber, A.L. (1984). Nonenzymatic formation of "energy-rich" lactoyl and glyceroyl thioesters from glyceraldehyde and a thiol. J. Mol. Evol. *20*, 157–166.
15. Raulin, F., Bloch, S., and Toupance, G. (1977). Addition reactions of malonic nitriles with

alkanethiol in aqueous solution: Prebiotic synthesis of iminothioesters. Orig. Life *8*, 247–257.
16. Miller, S.L., and Parris, M. (1964). Synthesis of pyrophosphate under primitive earth conditions. Nature *204*, 1248–1250.
17. Canavelli, P., Islam, S., and Powner, M.W. (2019). Peptide ligation by chemoselective aminonitrile coupling in water. Nature *571*, 546–549.
18. Gibard, C., Bhowmik, S., Karki, M., Kim, E.-K., and Krishnamurthy, R. (2018). Phosphorylation, oligomerization and self-assembly in water under potential prebiotic conditions. Nat. Chem. *10*, 212–217.
19. Herschy, B., Chang, S.J., Blake, R., Lepland, A., Abbott-Lyon, H., Sampson, J., Atlas, Z., Kee, T.P., and Pasek, M.A. (2018). Archean phosphorus liberation induced by iron redox geochemistry. Nat. Commun. *9*, 1346.
20. Hyde, A.S., and House, C.H. (2024). Prebiotic thiol-catalyzed thioamide bond formation. Geochem. Trans. *25*, 5.
21. De Duve, C. (1991). Blueprint for a Cell: The Nature and Origin of Life (Portland Press).
22. Bracher, P.J., Snyder, P.W., Bohall, B.R., and Whitesides, G.M. (2011). The relative rates of thiol–thioester exchange and hydrolysis for alkyl and aryl thioalkanoates in water. Orig. Life Evol. Biosph. *41*, 399–412.
23. Frenkel-Pinter, M., Rajaei, V., Glass, J.B., Hud, N.V., and Williams, L.D. (2021). Water and life: The medium is the message. J. Mol. Evol. *89*, 2–11.
24. Russell, M.J. (2021). The "water problem"(sic), the illusory pond and Life's Submarine Emergence—A Review. Life *11*, 429.
25. Sanden, S.A., Yi, R., Hara, M., and McGlynn, S.E. (2020). Simultaneous synthesis of thioesters and iron–sulfur clusters in water: two universal components of energy metabolism. Chem. Commun. *56*, 11989–11992.
26. Whicher, A., Camprubi, E., Pinna, S., Herschy, B., and Lane, N. (2018). Acetyl phosphate as a primordial energy currency at the origin of life. Orig. Life Evol. Biosph. *48*, 159–179.
27. Dawson, P.E., Muir, T.W., Clark-Lewis, I., and Kent, S.B. (1994). Synthesis of proteins by native chemical ligation. Science *266*, 776–779.
28. Breezee, J., Cady, N., and Staley, J.T. (2004). Subfreezing growth of the sea ice bacterium "psychromonas ingrahamii". Microb. Ecol. *47*, 300–304.
29. Takai, K., Nakamura, K., Toki, T., Tsunogai, U., Miyazaki, M., Miyazaki, J., Hirayama, H., Nakagawa, S., Nunoura, T., and Horikoshi, K. (2008). Cell proliferation at 122 degrees C and isotopically heavy CH4 production by a hyperthermophilic methanogen under high-pressure cultivation. Proc. Natl. Acad. Sci. USA *105*, 10949–10954.
30. DiGiacomo, J., McKay, C., and Davila, A. (2022). Thermobase: A database of the phylogeny and physiology of thermophilic and hyperthermophilic organisms. PLoS One *17*, e0268253.
31. Catchpole, R.J., and Forterre, P. (2019). The evolution of reverse gyrase suggests a nonhyperthermophilic last universal common ancestor. Mol. Biol. Evol. *36*, 2737–2747.
32. Forterre, P., Mirambeau, G., Jaxel, C., Nadal, M., and Duguet, M. (1985). High positive supercoiling *in vitro* catalyzed by an atp and polyethylene glycol-stimulated topoisomerase from sulfolobus acidocaldarius. EMBO J *4*, 2123–2128.
33. Kikuchi, A., and Asai, K. (1984). Reverse gyrase—a topoisomerase which introduces positive superhelical turns into DNA. Nature *309*, 677–681.
34. Slesarev, A.I. (1988). Positive supercoiling catalysed *in vitro* by atp-dependent topoisomerase from desulfurococcus amylolyticus. Eur. J. Biochem. *173*, 395–399.
35. Van Wazer, J.R., Griffith, E.J., and McCullough, J.F. (1955). Structure and properties of the condensed phosphates. vii. hydrolytic degradation of pyro-and tripolyphosphate. J. Am. Chem. Soc. *77*, 287–291.
36. Hulett, H.R. (1970). Non-enzymatic hydrolysis of adenosine phosphates. Nature *225*, 1248–1249.
37. Stockbridge, R.B., and Wolfenden, R. (2011). Enhancement of the rate of pyrophosphate hydrolysis by nonenzymatic catalysts and by inorganic pyrophosphatase. J. Biol. Chem. *286*, 18538–18546.
38. Chandru, K., Gilbert, A., Butch, C., Aono, M., and Cleaves, H.J. (2016). The abiotic chemistry of thiolated acetate derivatives and the origin of life. Sci. Rep. *6*, 29883.
39. Amend, J.P., and Shock, E.L. (2001). Energetics of overall metabolic reactions of thermophilic and hyperthermophilic archaea and bacteria. FEMS Microbiol. Rev. *25*, 175–243.
40. Hoehler, T., Alperin, M.J., Albert, D.B., and Martens, C.S. (2001). Apparent minimum free energy requirements for methanogenic archaea and sulfate-reducing bacteria in an anoxic marine sediment. FEMS Microbiol. Ecol. *38*, 33–41.
41. Schink, B. (1997). Energetics of syntrophic cooperation in methanogenic degradation. Microbiol. Mol. Biol. Rev. *61*, 262–280.
42. Martin, R.B. (1998). Free energies and equilibria of peptide bond hydrolysis and formation. Biopolymers *45*, 351–353.
43. Weber, A.L. (2004). Kinetics of organic transformations under mild aqueous conditions: implications for the origin of life and its metabolism. Orig. Life Evol. Biosph. *34*, 473–495.
44. Russell, M.J. (2003). Geochemistry. The importance of being alkaline. Science *302*, 580–581.
45. Russell, M.J. (2018). Green rust: The simple organizing 'seed'of all life? Life *8*, 35.
46. Wächtershäuser, G. (1990). Evolution of the first metabolic cycles. Proc. Natl. Acad. Sci. USA *87*, 200–204.
47. Keller, M., Blöchl, E., Wächtershäuser, G., and Stetter, K.O. (1994). Formation of amide bonds without a condensation agent and implications for origin of life. Nature *368*, 836–838.
48. Reanney, D.C. (1977). Aminoacyl thiol esters and the origins of genetic specificity. J. Theor. Biol. *65*, 555–569.
49. Miyakawa, S., Cleaves, H.J., and Miller, S.L. (2002). The cold origin of life: B. implications based on pyrimidines and purines produced from frozen ammonium cyanide solutions. Orig. Life Evol. Biosph. *32*, 209–218.
50. Price, P.B. (2007). Microbial life in glacial ice and implications for a cold origin of life. FEMS Microbiol. Ecol. *59*, 217–231.
51. Toner, J.D., and Catling, D.C. (2020). A carbonate-rich lake solution to the phosphate problem of the origin of life. Proc. Natl. Acad. Sci. USA *117*, 883–888.
52. Hao, J., Glein, C.R., Huang, F., Yee, N., Catling, D.C., Postberg, F., Hillier, J.K., and Hazen, R.M. (2022). Abundant phosphorus expected for possible life in Enceladus's ocean. Proc. Natl. Acad. Sci. USA *119*, e2201388119.
53. Postberg, F., Sekine, Y., Klenner, F., Glein, C.R., Zou, Z., Abel, B., Furuya, K., Hillier, J.K., Khawaja, N., Kempf, S., et al. (2023). Detection of phosphates originating from enceladus's ocean. Nature *618*, 489–493.
54. Shibuya, T., Komiya, T., Nakamura, K., Takai, K., and Maruyama, S. (2010). Highly alkaline, high-temperature hydrothermal fluids in the early archean ocean. Precambrian Res. *182*, 230–238.
55. Powner, M.W., Gerland, B., and Sutherland, J.D. (2009). Synthesis of activated pyrimidine ribonucleotides in prebiotically plausible conditions. Nature *459*, 239–242.
56. Kirk Nordstrom, D., Blaine McCleskey, R., and Ball, J.W. (2009). Sulfur geochemistry of hydrothermal waters in yellowstone national park: Iv acid–sulfate waters. Appl. Geochem. *24*, 191–207.
57. Franz, H.B., King, P.L., and Gaillard, F. (2019). Sulfur on mars from the atmosphere to the core. In Volatiles in the Martian crust (Elsevier), pp. 119–183.
58. Franz, H.B., McAdam, A.C., Ming, D.W., Freissinet, C., Mahaffy, P.R., Eldridge, D.L., Fischer, W.W., Grotzinger, J.P., House, C.H., Hurowitz, J.A., et al. (2017). Large sulfur isotope fractionations in martian sediments at gale crater. Nat. Geosci. *10*, 658–662.
59. Eigenbrode, J.L., Summons, R.E., Steele, A., Freissinet, C., Millan, M., Navarro-González, R., Sutter, B., McAdam, A.C., Franz, H.B., Glavin, D.P., et al. (2018). Organic matter preserved in 3-billion-year-old mudstones at gale crater, mars. Science *360*, 1096–1101.
60. Williams, N.H. (2000). Magnesium ion catalyzed atp hydrolysis. J. Am. Chem. Soc. *122*, 12023–12024.
61. Hoehler, T.M., and Jørgensen, B.B. (2013). Microbial life under extreme energy limitation. Nat. Rev. Microbiol. *11*, 83–94.
62. Lide, D.R. (2004). CRC Handbook of Chemistry and Physics, *85* (CRC press).
63. Wiberg, N. (2001). Holleman-wiberg's Inorganic Chemistry (Academic press).
64. Alberty, R.A., and Goldberg, R.N. (1992). Standard thermodynamic formation properties for the adenosine 5'-triphosphate series. Biochemistry *31*, 10610–10615.
65. King, D.W., and Kester, D.R. (1990). A general approach for calculating polyprotic acid speciation and buffer capacity. J. Chem. Educ. *67*, 932.
66. Jencks, W.P., Cordes, S., and Carriuolo, J. (1960). The free energy of thiol ester hydrolysis. J. Biol. Chem. *235*, 3608–3614.
67. Jencks, W.P., and Gilchrist, M. (1964). The free energies of hydrlysis of some esters and thiol esters of acetic acid. J. Am. Chem. Soc. *86*, 4651–4654.
68. da Silva, E.F., Svendsen, H.F., and Merz, K.M. (2009). Explicitly representing the solvation shell in continuum solvent calculations. J. Phys. Chem. A *113*, 6404–6409.
69. Fu, C.-W., and Lin, T.-H. (2011). Theoretical study on the alkaline hydrolysis of methyl thioacetate in aqueous solution. J. Phys. Chem. A *115*, 13523–13533.
70. Marenich, A.V., Cramer, C.J., and Truhlar, D.G. (2009). Universal solvation model based on solute electron density and on a continuum model of the solvent defined by the bulk dielectric constant and atomic surface tensions. J. Phys. Chem. B *113*, 6378–6396.

71. Ribeiro, A.J.M., Ramos, M.J., and Fernandes, P.A. (2010). Benchmarking of dft functionals for the hydrolysis of phosphodiester bonds. J. Chem. Theory Comput. *6*, 2281–2292.
72. Adamo, C., and Barone, V. (1999). Toward reliable density functional methods without adjustable parameters: The pbe0 model. J Chem Physics *110*, 6158–6170.
73. Sunner, S., and Wadsö, I. (1957). The heat of hydrolysis of thiolacetic acid. Trans. Faraday Soc. *53*, 455–459.
74. Wadso, I., Lothe, J., Lunde, K., Schliack, J., and Reio, L. (1957). The heats of hydrolysis of some alkyl thiolesters. Acta Chem. Scand. *11*, 1745–1751.
75. Pratt, L.S., and Reid, E.E. (1915). Studies in esterification. vi. the esterification of benzoic acid by mercaptans. J. Am. Chem. Soc. *37*, 1934–1948.
76. Alberty, R.A. (2003). Thermodynamics of the hydrolysis of adenosine triphosphate as a function of temperature, ph, pMg, and ionic strength. J. Phys. Chem. B *107*, 12324–12330.
77. George, P., Witonsky, R.J., Trachtman, M., Wu, C., Dorwart, W., Richman, L., Richman, W., Shurayh, F., and Lentz, B. (1970). "Squiggle-$H_2O$". an enquiry into the importance of solvation effects in phosphate ester and anhydride reactions. Biochim. Biophys. Acta *223*, 1–15.
78. Noor, E., Haraldsdóttir, H.S., Milo, R., and Fleming, R.M.T. (2013). Consistent estimation of gibbs energy using component contributions. PLoS Comput. Biol. *9*, e1003098.
79. Boeker, E.A. (1984). Simple integrated rate equations for reversible bimolecular reactions. Experientia *40*, 453–456.

## STAR★METHODS

### KEY RESOURCES TABLE

| REAGENT or RESOURCE | SOURCE | IDENTIFIER |
|---|---|---|
| Chemicals, peptides, and recombinant proteins | | |
| thioacetic acid, 96% | Sigma-Aldrich | 507-09-5 |
| S-methyl thioacetate, 95% | Sigma-Aldrich | 1534-08-3 |
| Citric Acid, 99% | Sigma-Aldrich | 77-92-9 |
| Deuterium Oxide | Sigma-Aldrich | 7789-20-0 |
| Deposited data | | |
| Hydrolysis rates of triphosphate | Van Wazer et al.[35] | |
| Hydrolysis rates of ATP | Hulett[36] | |
| Hydrolysis rates of diphosphate | Stockbridge and Wolfenden[37] | |
| Hydrolysis rates of thioacetic acid and methyl-thioacetate | Chandru et al.[38] | |
| Software and algorithms | | |
| Hydrolysis Model | Zenodo | https://doi.org/10.5281/zenodo.10801842 |
| MATLAB (R2021) | MathWorks | |
| Excel 365 | Microsoft | |

### METHOD DETAILS

#### Hydrolytic rate measurements

The hydrolysis rates for thioacetic acid (96%, Sigma-Aldrich) and S-methyl thioacetate (95%, TCI) were measured in a 100 mM, pH 5 citric acid buffer (Sigma-Aldrich, 99%, adjusted to pH 5 with 1 M NaOH) prepared with water obtained from a Milli-Q Integral 3 system (18.2 M Ω at 25°C). TAA or MTA were diluted 1:4 with $D_2O$ (99%, Sigma-Aldrich) to give a final concentration of 0.036 M prior to sealing the top of the tube with a Bunsen burner. The $^1H$ nuclear magnetic resonance (NMR) spectra were recorded with a Bruker AVANCE III 400 MHz spectrometer and a 5mm 1H/13C dual probe. After recording initial spectra, the samples were heated to the desired temperature (ranging from 50 - 80°C). To obtain the the free energy of activation and frequency factor for the hydrolysis of the respective compound, the measurement was conducted at 4 different temperatures with samples prepared as triplicates and a minimum of 13 measurement points were collected for each sample. The calculated free energies of activation and frequency factors of hydrolysis for all discussed compounds and their respective protonation states are summarized in Table S1.

#### Extrapolation of reaction kinetics

The hydrolysis rates of diphosphate, triphosphate and ATP were extracted from the literature[35–37] and a minimum of 3 measurements at different temperatures per studied pH were used to construct a hydrolysis rate equation that separates the hydrolysis rates of the individual protonation states ($k_i$) based on the inferred concentration ($\rho_i$) calculated from the respective pka values for each measured reaction rate at a certain pH:

$$k_{combined} = \sum_{i=1}^{j} \rho_i * k_i \quad \text{(Equation 1)}$$

The pKa values for diphosphate were taken from,[62] triphosphate from[63] and ATP were extracted from.[64] To calculate the concentrations of the individual protonation states, the degree of dissociation $\eta$ was determined using the following relation[65]:

$$\eta = \frac{\sum_{j=0}^{n}\left(\left(\prod_{i=0}^{j} K_i\right)[H^+]^{n-j}\right)}{\sum_{j=0}^{n}\left(\left(j\prod_{i=0}^{j} K_i\right)[H^+]^{n-j}\right)} \quad \text{(Equation 2)}$$

where j denotes the order of dissociation of for n protons and $K_i$ the reaction quotient for the dissociation of species i of compound A:

$$K_i = \frac{[H^+]\left[H_{n-j}A^{j-}\right]}{H_{n-j+1}A^{-j+1}} \quad \text{(Equation 3)}$$

## Thermochemistry using density functional theory

While the hydrolytic energies of acetyl-thioesters are constrained to -32.3 kJ $mol^{-1}$ for S-acetyl-mercaptopropanol and -31.5 kJ $mol^{-1}$ ( N-acetyl-$\beta$-mercaptoethylamine and Acetyl-Coenzyme A),[66,67] no experimental literature value for TAA was found. To obtain a consistent set of hydrolysis energies that includes MTA and TAA, the Gibbs free energies of hydrolysis were computed via DFT using PBE0 6-311(2d,2p) and the SMD solvation model including implicit solvation. Compounds with a net charge, such as the here considered deprotonated phosphoesters, are known to produce large errors in polarizable continuum models (PCM) with mean errors around 10 kcal/mol. Therefore, an implicit/explicit solvation scheme was employed,[68,69] in which four water molecules are placed in hydrogen bonding distance (ca. 1.5 - 2.5 Å) of the residues with the highest net charge. Based on the benchmarks of different PCM models, the best performing solute electron density continuum model (SMD) was chosen, which produces mean errors of 5 kcal/mol for the solvation energies of ionic species.[70] A benchmark of suitable density functionals for the hydrolysis of dimethyl-phosphate determined that PBE(0) is the most accurate hybrid functional with a generalized gradient approximation for thermochemistry and yields an improvement of about 2 kcal/mol over B3LYP,[71] therefore the free energies of hydrolysis determined in an earlier work were computed with PBE0 and a larger basis set.[38] The free energies of formation were thus calculated using the PBE(0) density functional and the 6-311G(2d,2p) basis set as implemented in *Guassian16 Rev. C.01*.[72] and to account for the solvation energies in water, the molecules were embedded in a polarizable solvent continuum (SMD).[70] The computed Gibbs free energies of hydrolysis of the respective chemical species are given in Table S2.

Comparing the $\Delta H$ for MTA and TAA found by Sunner & Wadso (which do not refer to dilute aqueous conditions and physiological pH), TAA is expected to yield less hydrolytic energy and is here computed with $\Delta G'_{pH7}$ -24.4 kJ $mol^{-1}$.[73,74] MTA is calculated to yield $\Delta G'_{pH7}$ = -29.8 kJ $mol^{-1}$ and lies close to the expected value of -32 kJ $mol^{-1}$ for thioesters in general. Slightly lower energy is expected due the influence of alkly chain length on thioester equilibria.[75] The computed values for PP and ATP also only deviate slightly from literature with $\Delta G'_{pH7}$ = - 11.1 kJ $mol^{-1}$ vs. -13.8 kJ $mol^{-1}$ for diphosphate and ATP with -40.8 $kJ^{-1}$ vs. -36.9 kJ $mol^{-1}$.[76] The Gibbs free energies of hydrolysis denoted herein as $\Delta G'_{pH7}$ are referring to 1 molar concentrations of reactants and products and 55.55 mol of water at pH 7 and 300 K.

Our calculations also include inorganic triphosphate, which is expected to yield comparable values to ATP, but with $\Delta G'_{pH7}$ = - 56.3 kJ $mol^{-1}$ the highly charged $HP_3O_{10}^{-4}$ species is likely subject to errors that are not accounted for by implicit and explicit solvation by SMD.[77] Similarly, $P_2O_7^{-4}$ with $\Delta G'_{pH7}$ = -36.7 kJ $mol^{-1}$ exceeds the expected -13.9 kJ $mol^{-1}$ based on the values given by Alberty et al., but an increase in free energy by -13.3 kJ $mol^{-1}$ from $HP_2O_7^{-3}$ to $P_2O_7^{-4}$ with $\Delta G'_{pH7}$ = -43.7 kJ $mol^{-1}$ was calculated by George et al.[77,78] Additional experimental measurements of hydroyltic energies under alkaline conditions would be required to determine, whether such an increase in hydrolysis energy for the -4 or higher charged species is indeed occurring due to an increase in solvation energy. With a $pK_a$ of 9.3 for $P_2O_7^{-4}$, the influence of this species is negligible at pH 9 and below. At pH 10, the initially provided free energy for $P_2O_7^{-4}$ and $HP_2O_7^{-3}$ is comparable to ATP with -41.9 and -38.9 kJ $mol^{-1}$ respectively (Figure S1).

## Hydrolysis model

The combined hydrolysis model assumes a closed, isothermal system without spatial gradients. To account for changes in hydrolysis rates and free energies depending on pH and temperature, the reaction rates and energies are computed as linear combinations of individual chemical species i.e. different protonation states of diphosphate. For the reaction rates of thioesters and thioacids, which are represented by only one chemical species between pH 5 and 10, two additional species are created at pH 5 and 10 to better reflect the reaction rates from the hydrolytic experiments. Using the measured hydrolysis rates, the reaction product concentrations at a given time point are determined using the integrated rate laws for pseudo-zero order reactions.[79] The reactant and product concentrations are then converted into hyrolytic energy using the computed Gibbs free energies from DFT.

If we assume that 1) the system is initialised with a certain concentration of $A$ and then closed and kept in an isothermal condition, 2) there is no fluid motion in the system, 3) the system is well mixed and thus has no spatial gradients of $A$ and 4) that a pseudo first order hydrolysis reaction $A -> P + Q$ is the only process that can decrease the concentration of $A$, the changes in product concentration can be described as:

$$\frac{\partial P}{\partial t} = k_1 \frac{PQ - A}{K_e} \quad \text{(Equation 4)}$$

where $k_1$ corresponds to the forward rate of reaction and $K_e$ the equilibrium constant, respectively. Solving the integrated rate laws derived by Boeker for the product concentration $P_t$ at time point $t$,[79] the following relation is obtained (Equation 5 below):

$$P_t = \frac{P_o - \left(2 * P_e * P_o + P_e^2 * exp(\alpha + P_o^2 * exp(\alpha - P_e^2 - P_o^2 - D * P_e + D * P_o + D * P_e * exp(\alpha - D * P_o * exp(\alpha - 2 * P_e * P_o * exp(\alpha)\right)}{D + P_e - P_o - P_e * exp(\alpha) + P_o * exp(\alpha)}$$

(Equation 5)

with $\alpha$ and the discriminant $D$ corresponding to

$$\alpha = (D * k_1 * t) / K_e \quad \text{(Equation 6)}$$

$$D = -\sqrt{(P_o + Q_o + K_e)^2 + 4(K_e * A_o - P_o * Q_o)} \quad \text{(Equation 7)}$$

where the subscript *o* refers to the initial concentration of reactants and products, the subscript *e* refers to the concentration of reactant and products at equilibrium. The concentration of $P_e$ was calculated with the vpa numerical solver of MATLAB solving for $X$, which represents the hydrolyzed compound A, using the relation:

$$K_e = \frac{(X+P_o)^2}{((A_o - X) * \rho_{H_2O}} \quad \text{(Equation 8)}$$

$P_e$ then equals $X + P_o$ to account for the initial, molar concentration of the product in mol/L, when $\rho_{H_2O} = 55.555$. The free energy of the reaction is given by:

$$\Delta G(t) = \Delta G_0 + RT \ln \frac{P_t^2}{A_o - P_t + P_o * \rho_{H_2O}} \quad \text{(Equation 9)}$$

As to also incorporate the temperature dependence of the hydrolysis rates and Gibbs free energies, both the hydrolysis rates and free energies were input as vectors, with $P_e$ also being recalculated using Equation 8 as to account for changes in the entropy of reaction.

## QUANTIFICATION AND STATISTICAL ANALYSIS

The Microsoft Excel 365 function LINEST was used to perform the regression from the measured hydrolysis rates to the tabulated reaction rate parameters (Table S1 and Figure 1). The goodness of fit was determined by the coefficent of determination of the residual sum of squares method, which exceeded a value of 0.99, except for MTA at pH 5, for which a $r^2$ of 0.56 was obtained after triplicate measurements.